IEEE Access
Multidisciplinary : Rapid Review : Open Access Journal

Received April 30, 2018, accepted May 25, 2018, date of publication June 4, 2018, date of current version June 29, 2018.

Digital Object Identifier 10.1109/ACCESS.2018.2843774

Dynamic Similar Sub-Series Selection Method for Time Series Forecasting

PEIQIANG LI[1], JIANG ZHANG[1,2], CANBING LI[1,2], (Senior Member, IEEE), BIN ZHOU[1,2], (Senior Member, IEEE), YONGJUN ZHANG[3], MANMAN ZHU[1,2], AND NING LI[1,2]

[1]College of Electrical and Information Engineering, Hunan University, Changsha 410082, China
[2]Hunan Key Laboratory of Intelligent Information Analysis and Integrated Optimization for Energy Internet, Hunan University, Changsha 410082, China
[3]School of Electric Power, South China University of Technology, Guangzhou 510640, China

Corresponding author: Canbing Li (lcb@hnu.edu.cn)

This work was supported by the Sino-US International Science and Technology Cooperation Project under Grant 2016YFE0105300.

ABSTRACT Accumulation of influencing factors during several consecutive time periods makes the variation of target parameters lag behind the variation of their influencing factors. This important phenomenon, known as the cumulative effect, would lead to relatively large forecasting errors. In this paper, the dynamic similar sub-series method is proposed to take cumulative effect into consideration. The similar sub-series for the forecasting parameter sub-series are selected based on similarities of target parameter sub-series and influencing factors sub-series. The internal variations of target parameter sub-series and each influencing factor sub-series are innovatively integrated into the selection rules for the dynamic similar sub-series. The corresponding forecasting algorithm is designed, and the forecasting parameters are deduced and forecasted according to the variation of the dynamic similar sub-series. The proposed method is compared with a variety of representative methods under the short-term daily average load forecasting, the electricity price forecasting and the global horizontal irradiance forecasting scenarios to demonstrate its effectiveness.

INDEX TERMS Forecasting method, time series, cumulative effect, short-term daily average load, electricity price.

I. INTRODUCTION

Forecasting plays a vital role in decision-making process, and it has been extensively applied in various fields, such as finance, physics, engineering, and mathematics [1]–[4]. The general purpose of forecasting is to establish a mathematical model that can forecast the future observations based on historical recorded data [5], [6].

It is generally assumed that the impact of influencing factors on the target parameters will persist into the foreseeable future. Many forecasting algorithms, such as time series method [7], [8], autoregressive integrated moving average (ARIMA) [9], particle swarm optimization (PSO) [10], support vector machine (SVM) [11], and artificial neural networks (ANN) [12], have been widely utilized and improved. Hybrid forecasting methods have been widely applied to both long-term and short-term forecasting systems in recent years [13]–[15]. In [16], a hybrid method based on the wavelet transform, PSO, and adaptive-network-based fuzzy inference system (ANFIS) was proposed to forecast short-term electricity price under the electricity market of mainland Spain. Two hybrid methods (ARIMA-ANN and ARIMA-SVM) were respectively utilized to predict the wind speed and wind power generation time series in [17]. As one of the basic methods of forecasting, time series method is extensively used in the energy field. In order to forecast the next period of time series, many single and hybrid forecasting methods were proposed and used to predict power load [18]–[20], electricity price [21]–[23], wind power [24]–[26], and etc.

The forecasting parameters are variables in the target parameters that require to be forecasted based on historical recorded data. Historical recorded data include target parameters and different influencing factors. Because of complex influences different influencing factors exert on the forecasting parameters, various influencing factors are required to be taken into consideration in time series forecasting. Generally, the forecasting parameters were merely deduced and obtained by the weighted average of the target parameters in previous several time periods, which would unable meet the requirements for improving the forecasting accuracy [27]. The general rule to select similar time series is to find one or several

Time	...	t_1	t_2	t_3	t_4	...	$t_{i\text{-}3}$	$t_{i\text{-}2}$	$t_{i\text{-}1}$	t_i	...	$t_{n\text{-}3}$	$t_{n\text{-}2}$	$t_{n\text{-}1}$	t_n
Influencing factors (1)	...	$I_{1.1}$	$I_{1.2}$	$I_{1.3}$	$I_{1.4}$	...	$I_{1.i\text{-}3}$	$I_{1.i\text{-}2}$	$I_{1.i\text{-}1}$	$I_{1.i}$	...	$I_{1.n\text{-}3}$	$I_{1.n\text{-}2}$	$I_{1.n\text{-}1}$	$I_{1.n}$
Influencing factors (2)	...	$I_{2.1}$	$I_{2.2}$	$I_{2.3}$	$I_{2.4}$	...	$I_{2.i\text{-}3}$	$I_{2.i\text{-}2}$	$I_{2.i\text{-}1}$	$I_{2.i}$	...	$I_{2.n\text{-}3}$	$I_{2.n\text{-}2}$	$I_{2.n\text{-}1}$	$I_{2.n}$
⋮	⋮	⋮	⋮	⋮	⋮	⋮	⋮	⋮	⋮	⋮	⋮	⋮	⋮	⋮	⋮
Influencing factors (C)	...	$I_{C.1}$	$I_{C.2}$	$I_{C.3}$	$I_{C.4}$	...	$I_{C.i\text{-}3}$	$I_{C.i\text{-}2}$	$I_{C.i\text{-}1}$	$I_{C.i}$	...	$I_{C.n\text{-}3}$	$I_{C.n\text{-}2}$	$I_{C.n\text{-}1}$	$I_{C.n}$
Target parameters	...	L_1	L_2	L_3	L_4	...	$L_{i\text{-}3}$	$L_{i\text{-}2}$	$L_{i\text{-}1}$	L_i	...	$L_{n\text{-}3}$	$L_{n\text{-}2}$	$L_{n\text{-}1}$	L_n

Forecasting parameters

FIGURE 1. Cumulative effect of influencing factors on target parameters.

target parameters whose corresponding influencing factors are similar to the influencing factors of the forecasting parameters to some extent. In addition, linear and nonlinear fitting formulas are extensively used to select the similar time series. However, methods of this kind are susceptible to the cumulative effect, which would lead to a substantial forecasting error. Therefore, a more reasonable and appropriate similar series selection method plays a decisive role in time series forecasting.

The cumulative effect is widely found and considered in time series forecasting. For example, the cumulative effect of temperature was considered in short-term load forecasting (STLF) in [28]. The general mechanism of the cumulative effect of temperature in the power system load forecast was described in [28] and [29]. The cumulative effect coefficients at different temperatures were obtained and the temperatures were revised to reflect the cumulative effect. However, the impact of different temperature differences on the cumulative effect of temperature was not discussed. Thus, if the dynamic features of the variation of the time series could be appropriately taken into consideration, it will be more conducive to truly reflect the essence of the cumulative effect.

Contributions in this paper can be summarized as follows:

1) In order to reflect the effect of the cumulative effect in similar time series selection as accurately as possible and thus make well-performed forecasting, the dynamic similar sub-series method is proposed in this paper. The dynamic similar sub-series for the forecasting parameter sub-series are selected based on similarities of target parameter sub-series and influencing factors sub-series. The internal variations of target parameter sub-series and each influencing factor sub-series are innovatively integrated into the selection rules for the dynamic similar sub-series.

2) The corresponding forecasting algorithm is designed according to the variation of the dynamic similar sub-series, which ensures the proposed method's capacity for being separately implemented for time series forecasting. In addition, the method proposed in this paper can also be used as a basis for selecting similar sub-series and thus hybrid forecasting method can be formed when combined with other forecasting algorithms.

3) The proposed method has been compared with various representative approaches: ARIMA, Levenberg-Marquardt

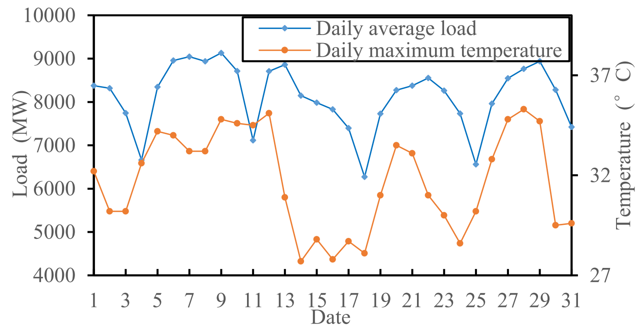

FIGURE 2. The variation curves of the daily maximum temperature and the daily average load.

algorithm neural network (LM-NN), back propagation neural network (BPNN) and back propagation through time (BPTT), under the short-term daily average load forecasting, the electricity price forecasting and the GHI forecasting scenarios. All results demonstrate that the proposed method outperforms the aforementioned approaches in terms of forecasting accuracy.

The rest of this paper is organized as follows. In Section II, the dynamic similar sub-series method is proposed. The forecasting algorithm and complete forecasting model are given in section III. Cases study is carried out in Section IV. Finally, this paper is summarized in Section V.

II. DYNAMIC SIMILAR SUB-SERIES METHOD

A. INFLUENCE OF CUMULATIVE EFFECT ON TIME SERIES FORECASTING

The cumulative effect refers to that the influencing factors of the several time periods before may have fairly obvious impacts on the forecasting parameters. As shown in Fig. 1, the historical data are recorded from time t_1 to time t_{n-1}, and C denotes the number of the influencing factors. Influencing factors at time t_n can be predicted and obtained from the additional external inputs. Due to the cumulative effect, the forecasting parameters L_n are not only related to the current influencing factors at time t_n, but also related to the influencing factors shortly before t_n. Such as, the influencing factors (2) at time t_{n-2} (i.e., $I_{2,n-2}$) may have more or fewer effects on the value of L_n.

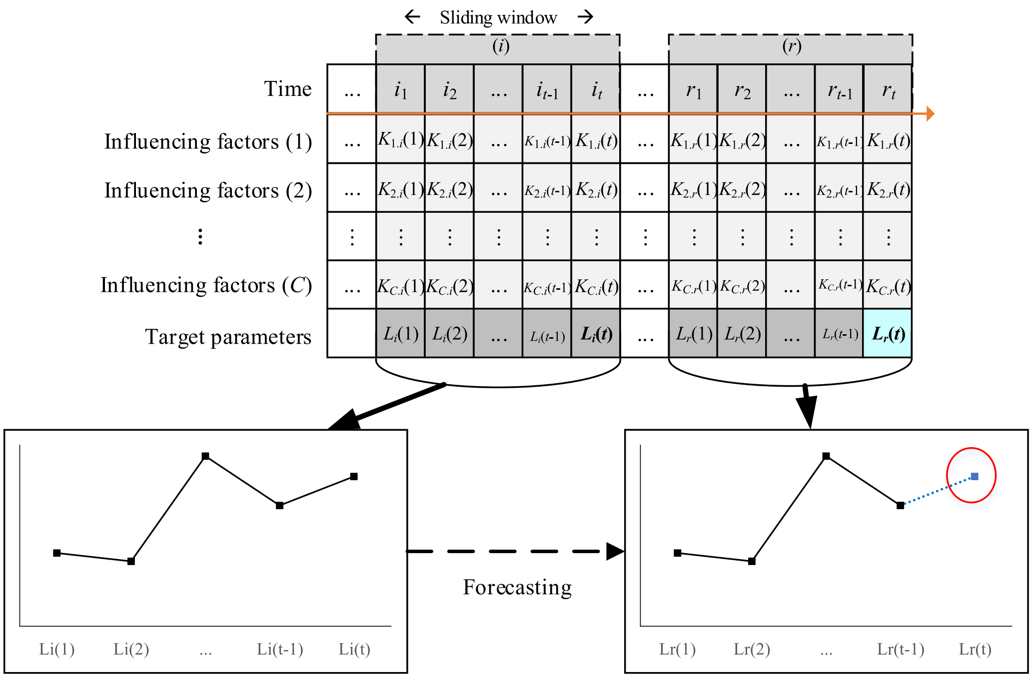

FIGURE 3. Schematic diagram of dynamic similar sub-series.

When relatively strong cumulative effect exists in time series forecasting, especially when there are continuous extreme values in the influencing factors, the forecasting parameters are easily affected by the variation of influencing factors several consecutive time periods before. For example, in load forecasting, the variation curves of the daily maximum temperature and the daily average load of a city in Guangdong, China in August 2013 are shown in Fig. 2. It can be observed that the overall variation of the daily maximum temperature is similar with the variation of the daily average load. When the daily maximum temperature rises, the daily average load will generally increase. However, after the end of several consecutive days of high temperatures, the daily average load still increased on August 13th.

The cumulative effect makes the variation of target parameters lags behind the variation of their influencing factors. Therefore, in a system which exists cumulative effect, even in the case of two moments which have identical external influencing factors, the target parameters may also be substantially different.

B. DYNAMIC SIMILAR SUB-SERIES

In this subsection, the idea of dynamic similar sub-series is proposed to select similar sub-series for the forecasting parameter sub-series. In the following, details of the dynamic similar sub-series are described.

Given the data recorded in the past, from time t_1 to time t_{n-1}, this study aims at forecasting the target parameters at time t_n (i.e., the forecasting parameters). For target parameters, r sub-series of the target parameters can be generated in turn by sliding window with the length of $W-1$, where $r = n - W + 1$. $W-1$ consecutive target parameters before the forecasting parameters and $W-1$ consecutive target parameters before a certain time in history can form the following two time sub-series.

$$L_r = \{L_r(1), L_r(2), \ldots, L_r(W-1)\} \tag{1}$$
$$L_i = \{L_i(1), L_i(2), \ldots, L_i(W-1)\} \tag{2}$$

where L_r and L_i are the forecasting parameter sub-series and the ith target parameter sub-series, respectively, $i = 1, 2, \ldots, r-1$, the length of the window W depends on the duration of the cumulative effect, and it is a parameter to be determined.

For influencing factors, C influencing factors are taken into account. Influencing factors of forecasting parameters can be obtained through external system. In a parallel manner, for the cth influencing factor, where $c = 1, 2, \ldots, C$, r influencing factors sub-series can be generated by sliding window with the length of W.

$$K_{c.r} = \{K_{c.r}(1), K_{c.r}(2), \ldots, K_{c.r}(W)\} \tag{3}$$
$$K_{c.i} = \{K_{c.i}(1), K_{c.i}(2), \ldots, K_{c.i}(W)\} \tag{4}$$

where $K_{c.r}$ is the cth influencing factor sub-series corresponding to the forecasting parameter sub-series, $K_{c.i}$ is the cth influencing factor sub-series corresponding to the ith target parameter sub-series.

The dynamic similar sub-series means that the variation of the target parameter sub-series and their corresponding influencing factors sub-series in a similar historical series are considered to be similar to what is in the forecasting parameter sub-series and their corresponding influencing factors sub-series. As shown in Fig. 3, L_i is regarded as the dynamic similar sub-series of L_r. For example, in load forecasting, the idea of the dynamic similar sub-series is to find a historical sub-series whose variation of the daily average load and the daily features (such as weekday index and meteorological factors) are similar to the forecasting parameter sub-series'.

C. DYNAMIC SIMILARITY

In this subsection, the dynamic similarity is proposed in order to quantify the degree of similarity between two different sub-series. According to the difference of the objects, the dynamic similarities are divided into the dynamic similarity of target parameter sub-series and the dynamic similarities of influencing factors sub-series.

Due to the fact that different influencing factors have various forms and different scales, it is essential to quantify and unify each of the influencing factors before calculating. The variation curves of the target parameters and one of the influencing factors are shown in Fig. 4. For target parameter sub-series, the values of the target parameters vary greatly over time, especially for some rapidly-developing regions or industries. Therefore, only the variation in the target parameter sub-series needs to be considered and calculated. While for influencing factors sub-series, due to the influence of different values of influencing factors on the target parameters are different, not only the variation, but also the values of the influencing factors need to be considered.

The Euclidean Distance is a well-known distance function which can be used to indicate the difference of two vectors [30]. Two transformative functions of the Euclidean Distance are used in order to adapt to this work. Let $d_{L.i}$ be the difference degree of the rates of variation between L_i and L_r, and $d_{c.i}$ be the difference degree of the variation between $K_{c.i}$ and $K_{c.r}$. $d_{L.i}$ and $d_{c.i}$ can be respectively expressed by the following functions [30],

$$d_{L.i} = \frac{\sqrt{\sum_{u=1}^{W-2}\left[\frac{L_i(u+1)-L_i(u)}{L_i(u)} - \frac{L_r(u+1)-L_r(u)}{L_r(u)}\right]^2}}{W-2} \quad (5)$$

$$d_{c.i} = \frac{\sqrt{\sum_{v=1}^{W}\left[\frac{x_{c.i}(v)-x_{c.r}(v)}{x_{c.r}(v)}\right]^2}}{W} \quad (6)$$

where $L_i(u)$ and $L_r(u)$ are the uth target parameter in the target parameter sub-series L_i and L_r, respectively, $x_{c.i}(v)$ and $x_{c.j}(v)$ are the vth unified values of $K_{c.i}$ and $K_{c.r}$, respectively, and $x_{c.j}(W)$ is the unified value of the cth influencing factor.

The dynamic similarity of target parameter sub-series $S_{L.i}$ and the cth dynamic similarity of influencing factors sub-series $S_{c.i}$ can be obtained by the normalization equations, respectively, which are [30],

$$S_{L.i} = 1 - \frac{d_{L.i} - \min(d_{L.i})}{\max(d_{L.i}) - \min(d_{L.i})} \quad (7)$$

$$S_{c.i} = 1 - \frac{d_{c.i} - \min(d_{c.i})}{\max(d_{c.i}) - \min(d_{c.i})} \quad (8)$$

where $\max(d_{L.i})$ and $\min(d_{L.i})$ denote the maximum and minimum values of $d_{L.i}$, respectively, $\max(d_{c.i})$ and $\min(d_{c.i})$ denote the maximum and minimum values of $d_{c.i}$, respectively, $i = 1, 2, \ldots, r-1$.

D. METHODS FOR SELECTING DYNAMIC SIMILAR SUB-SERIES

The purpose of this subsection is to select similar sub-series for the forecasting parameter sub-series by applying the dynamic similar sub-series method. In this study, two methods are used: by weighted sum method and by fuzzy clustering method.

1) BY WEIGHTED SUM METHOD

The comprehensive dynamic similarity is defined firstly, which gives weights to the dynamic similarity of the target parameter sub-series and each influencing factor sub-series. The comprehensive dynamic similarity O_i can be expressed as,

$$\begin{cases} O_i = \beta_0 S_{L.i} + \sum_{c=1}^{C} \beta_c S_{c.i} \\ \beta_0 + \sum_{c=1}^{C} \beta_c = 1, \quad \beta_0, \beta_c > 0 \end{cases} \quad \text{with } i = 1, 2, \ldots, r-1 \quad (9)$$

where β_0 denotes the weight of the dynamic similarity of target parameter sub-series, β_c denotes the weight of the dynamic similarity of the cth influencing factor sub-series.

β_0 and β_c can be obtained by using the least square estimation (LSE) to optimize the dynamic similarity of target parameter sub-series, the dynamic similarities of influencing factors sub-series and the comprehensive dynamic similarity through the historical test dataset. Notice that, the optimization function is an implicit function of the discrete variables β_0 and β_c. Searching for the optimal solution will be extremely difficult. Thus, the fuzzy clustering method for the dynamic similar sub-series is designed and recommended in this study.

2) BY FUZZY CLUSTERING METHOD

Fuzzy clustering is a mathematical method to carry out classification analysis according to the relationship of the affinity degree and the similarity degree between different objects [31], [32]. $L = \{L_1, L_2, \ldots, L_n\}$ denotes a sample set of historical data consisting of n samples. In this study, the dynamic similarity of target parameter sub-series and the dynamic similarities of influencing factors sub-series are chosen as the characteristic indexes. D characteristic indexes in each historical sample can be obtained, where $D = C + 1$. The characteristic indexes of sample S_i can be expressed as follows,

$$S_i = (S_{L.i}, S_{1.i}, S_{2.i}, \ldots, S_{C.i})^T = (a_{1i}, a_{2i}, \ldots, a_{Di})^T \quad (10)$$

Then the characteristic matrix $\mathbf{I}$ for sample S_i can be established as follows,

$$\mathbf{I} = \begin{pmatrix} a_{11} & a_{12} & \cdots & a_{1j} \\ a_{21} & a_{22} & \cdots & a_{2j} \\ \vdots & \vdots & \cdots & \vdots \\ a_{D1} & a_{D2} & \cdots & a_{Dj} \end{pmatrix} \tag{11}$$

The similarity relations between each data sample are calculated after establishing the characteristic matrix $\mathbf{I}$. Let r_{ij} be the similarity degree of $S_i = (a_{1i}, a_{2i}, \ldots, a_{Di})$ and $S_j = (a_{1j}, a_{2j}, \ldots, a_{Dj})$. The fuzzy similarity matrix can be expressed as follows,

$$\mathbf{R} = \begin{pmatrix} r_{11} & r_{12} & \cdots & r_{1j} \\ r_{21} & r_{22} & \cdots & r_{2j} \\ \vdots & \vdots & \ddots & \vdots \\ r_{j1} & r_{j2} & \cdots & r_{jj} \end{pmatrix} \tag{12}$$

Plenty of methods can determine the similarity between two objects represented as vectors. In this work, the cosine similarity formula for D-dimensional vectors is used to compute the similarity of fuzzy similarity matrix [33],

$$r_{ij} = 1 - \frac{\sum_{k=1}^{D} [x_{ik} - E(S_i)] \cdot [x_{jk} - E(S_j)]}{\sqrt{\sum_{k=1}^{D} [x_{ik} - E(S_i)]^2 \cdot \sum_{k=1}^{D} [x_{jk} - E(S_j)]^2}} \tag{13}$$

where $E(S_i)$ and $E(S_j)$ are the mathematical expectations of S_i and S_j, respectively.

Finally, the transitive closure matrix $\mathbf{R}^* = t(\mathbf{R})$ is obtained by successive squares method, and after the appropriate confidence level $\lambda \in [0,1]$ is classified, each weight can be determined and the similar sub-series of the forecasting parameter sub-series can be found and selected.

III. TIME SERIES FORECASTING MODEL

A. FORECASTING ALGORITHM

After selecting the dynamic similar sub-series, the forecasting parameters can be forecasted based on the variation of the target parameters in dynamic similar sub-series and the forecasting parameter sub-series. In this study, the rate of variation of $L_r(W)$ relative to $L_r(W-1)$ is deemed to be approximately equal to the rate of variation of $L_i(W)$ relative to $L_i(W-1)$. Thus, the forecasting parameters $L_r(W)$ can be forecasted by the following equation,

$$\hat{L}_r(W) = \frac{L_i(W) \cdot L_r(W-1)}{L_i(W-1)} \tag{14}$$

where $\hat{L}_r(W)$ is the forecasted value of $L_r(W)$.

The relative error between the forecasted value $\hat{L}_r(W)$ and the actual value $L_r(W)$ can be expressed as,

$$\varepsilon_W = \frac{\hat{L}_r(W) - L_r(W)}{L_r(W)} \tag{15}$$

The relative error ε_W varies according to the selected dynamic similar sub-series. ε_W is thought to be approximately equal to the average relative errors of the rate of variation of the previous $W-1$ target parameters.

$$\begin{aligned} \bar{\varepsilon}_W &= \frac{1}{W-2} \sum_{b=2}^{W-1} \left[\frac{L_r(b) - L_r(b-1)}{L_r(b-1)} - \frac{L_i(b) - L_i(b-1)}{L_i(b-1)} \right] \\ &= \frac{1}{W-2} \sum_{b=2}^{W-1} \left[\frac{L_r(b)}{L_r(b-1)} - \frac{L_i(b)}{L_i(b-1)} \right] \end{aligned} \tag{16}$$

$$\varepsilon_W \approx \bar{\varepsilon}_W \tag{17}$$

where $\bar{\varepsilon}_W$ is the average relative errors of the rate of variation of the previous $W-1$ target parameters.

Therefore, the forecasting parameters can be obtained by the following equation,

$$L_r(W) = \frac{L_i(W) \cdot L_r(W-1)}{L_i(W-1) \cdot (\bar{\varepsilon}_W + 1)} \tag{18}$$

B. FORECASTING MODEL

In order to perform time series forecasting by using the selected dynamic similar sub-series, a complete forecasting model is given in this subsection. The forecasting model includes: 1) data acquisition, 2) additional inputs, 3) dynamic similar sub-series method, and 4) forecasting algorithm. In the following, more detailed descriptions are given.

- *Data acquisition:* The historical target parameters and corresponding different influencing factors are acquired from the memorizer.
- *Additional inputs:* If possible, the future information of the influencing factors can be obtained through the external systems.
- *Dynamic similar sub-series method:* By selecting the length of the window and sliding the window, the historical target parameters and corresponding different influencing factors are changed into sub-series. Dynamic similar sub-series of the forecasting parameter sub-series are found by the dynamic similar sub-series method.
- *Forecasting algorithm:* The forecasting algorithm is used to forecast the forecasting parameters with the obtained dynamic similar sub-series.

C. DETERMINING THE SIZE OF THE WINDOW

The selection of the size of the window (the value of W) depends on the duration of the cumulative effect in the case under study. Thus, adequate training datasets are required to be performed in order to find an appropriate value of W before applying to the time series forecasting.

Mathematically, when applying the proposed model to the training datasets, the value of W is determined by minimizing the forecasting errors. In this paper, the average absolute percentage error (MAPE) is adopted to evaluate the forecasting errors, which is,

$$MAPE = 100 \cdot \frac{1}{N} \sum_{h=1}^{N} \left| \frac{\hat{X}(h) - X(h)}{X(h)} \right| \tag{19}$$

where $\hat{X}(h)$ is the forecasted value for time h, which can be obtained from the proposed forecasting model, $X(h)$ is the actual recorded value, and N denotes the number of forecasted objects in training datasets.

Note that, W is a positive integer, and its value is not too large either. Therefore, an adequate value of W can be found without too many attempts.

$$W = \arg\min \{MAPE\} \tag{20}$$

New data can be added as part of the training datasets to reassess the size of the window. However, when the development processes of the time series is relatively stable, that is, if there is no major event or accident to have a continuous impact on the variation of the time series, it is only required to periodically reassess the size of the window as planned. Conversely, if there are some major events and accidents to have a continuous impact on the variation of the time series, these new data are required to be added to the test datasets and the size of the window are suggested to be reassessed in a timely manner.

IV. CASES STUDY

In order to validate the accuracy of the proposed method, the proposed method is compared with four representative approaches: ARIMA [34], LM-NN [12], BPNN [35] and BPTT [36]. These methods are utilized for short-term daily average load forecasting, electricity price forecasting and GHI forecasting, respectively.

Data for short-term daily average load forecasting come from a regional power grid in Guangdong, China. The ISO New England electricity prices are analyzed in electricity price forecasting [37]. In GHI forecasting, data from Nevada Power Clark Station (NPCS), Las Vegas, Nevada are analyzed [38].

In order to ensure the reliability of the comparison test, in the algorithm of LM-NN, BPNN and BPTT, the historical data from January 1st 2012 to the day before the forecasted day are used as the training samples when forecasting daily average load of the year 2014. In the meanwhile, when forecasting electricity price of the year 2008, the historical data from January 1st 2005 to the day before the forecasted day are used as the training samples. When forecasting GHI at 12 o'clock of the year 2014, the training samples comprise the historical data from January 1st 2007 to the day before the forecasted day.

A. SELECTING THE LENGTH OF THE WINDOW

By setting different lengths of the window (the value of W) and making tentative forecasting by using the testing datasets, MAPE for different values of W can be obtained. The results for short-term daily average load forecasting, electricity price forecasting and GHI forecasting are shown in Table 1, Table 2 and Table 3, respectively.

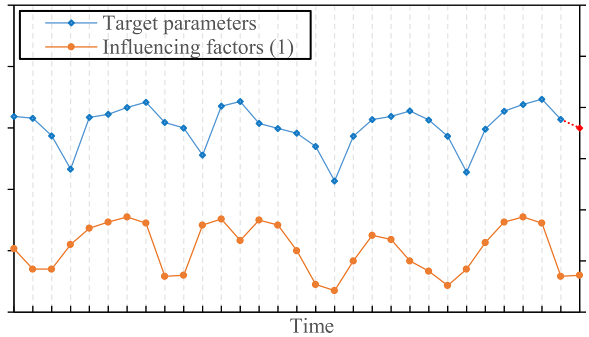

FIGURE 4. Target parameter sub-series and influencing factors sub-series variation curves.

TABLE 1. MAPE for the values of W (daily average load).

W	MAPE	W	MAPE
2	7.471%	6	2.070%
3	2.284%	7	2.209%
4	**1.883%**	8	2.445%
5	1.937%	9	2.302%

TABLE 2. MAPE for the values of W (electricity price).

W	MAPE	W	MAPE
2	16.428%	7	6.880%
3	12.401%	8	9.327%
4	10.255%	9	9.712%
5	8.951%	10	9.133%
6	**6.724%**	11	8.596%

TABLE 3. MAPE for the values of W (GHI).

W	MAPE	W	MAPE
2	10.307%	5	12.064%
3	**9.532%**	6	13.012%
4	10.498%	7	12.197%

It can be understood that the daily average loads are sensitive to the cumulative effect of influencing factors within 4 days. Thus, the value of W in short-term daily average load forecasting is set to 4. In a parallel manner, the value of W in electricity price forecasting and GHI forecasting are set to 6 and 3, respectively.

B. SHORT-TERM DAILY AVERAGE LOAD FORECASTING

In this case, the short-term daily average load forecasting model performs a day-ahead average load forecast, and the forecasting is mainly based on historical load and weather information. The structure of the forecasting model applied in the short-term daily average load forecasting is shown in Fig. 5.

In data acquisition, weekday index and weather information make up the data of the influencing factors.

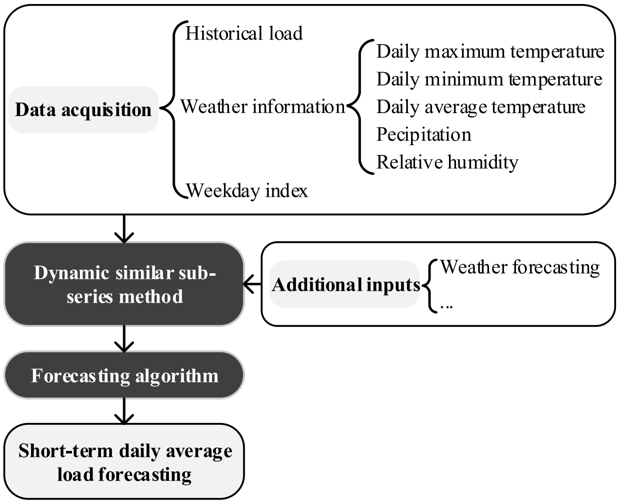

FIGURE 5. Short-term daily average load forecasting model.

TABLE 4. Weight for each parameters (daily average load).

Parameter	Weight	Parameter	Weight
β_0	0.00435	β_4	0.00074
β_1	0.00136	β_5	0.00057
β_2	0.00148	β_6	0.99
β_3	0.00150		

Weather information used in this study includes daily maximum temperature, daily minimum temperature, daily average temperature, precipitation, and relative humidity. In additional inputs, future weather information can be obtained through the local meteorological department, or the power micro-weather station.

When determining the weights of each sub-series, the weekday indexes of the dynamic similar sub-series are suggested to be the same or as possible as the weekday indexes of the forecasted sub-series. Therefore, the weight of the weekday index sub-series is set to 0.99 in advance. The fuzzy similarity matrix **R** formed by other sub-series is shown as follows:

$$\mathbf{R}=\begin{pmatrix} 1 & 0.660 & 0.704 & 0.707 & 0.121 & 0.089 \\ 0.660 & 1 & 0.913 & 0.958 & 0.129 & 0.013 \\ 0.704 & 0.913 & 1 & 0.984 & 0.310 & 0.099 \\ 0.707 & 0.958 & 0.984 & 1 & 0.215 & 0.065 \\ 0.121 & 0.129 & 0.310 & 0.215 & 1 & 0.364 \\ 0.089 & 0.013 & 0.099 & 0.065 & 0.364 & 1 \end{pmatrix} \tag{21}$$

Then each of the weights is calculated, and the result is presented in Table 4.

The MAPE obtained for every month in 2014 is presented in Table 5. It can be observed that the proposed method carries out the best forecasts in most months. The LM-NN and the BPNN excel the proposed method just in February 2014 and October 2014 (2.266% and 2.564% for LM-NN, 2.790% and 2.494% for BPNN versus 3.059% and 2.735% for the proposed method, respectively), and the BPTT performs better than the proposed method just in May 2014. Notice that, these MAPE obtained by the proposed method is not significantly high. In addition, the proposed method overcomes all of the representative approaches in average MAPE.

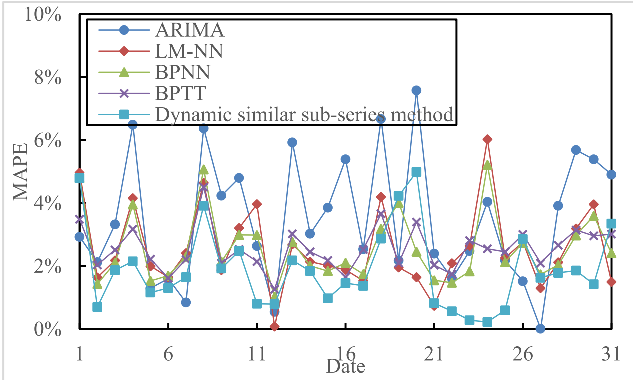

FIGURE 6. MAPE for August 2014 (daily average load).

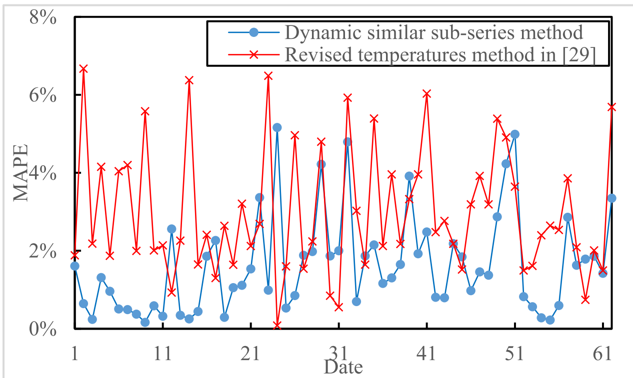

FIGURE 7. MAPE for July-August 2014 (daily average load).

The MAPE obtained by the aforementioned methods in August 2014 is shown in Fig. 6. In [29], several consecutive days of revised temperatures are used to take cumulative effect into account when forecasting summer power load. The MAPE obtained by the proposed method and [29] from July 2014 to August 2014 is shown in Fig. 7. It can be observed from Fig.6 and Fig.7 that the MAPE obtained by the proposed method is the lowest in most of the days. Therefore, remarkable enhancements can be intuitively observed from the proposed method in forecasting short-term daily average load time series.

C. ELECTRICITY PRICE FORECASTING

Hourly day-ahead electricity price forecasting is performed in this case. The structure of the electricity price forecasting model is shown in Fig. 8.

The data acquisition comprises historical electricity price, historical load, temperature information (dry bulb and dew point), historical natural gas price, and weekday index.

TABLE 5. Monthly MAPE in 2014 (daily average load).

Month	ARIMA	LM-NN	BPNN	BPTT	Dynamic similar sub-series method
Jan.	3.492%	2.551%	2.238%	2.580%	**2.217%**
Feb.	4.291%	**2.266%**	**2.790%**	3.471%	3.059%
Mar.	1.989%	2.037%	2.167%	1.707%	**1.561%**
Apr.	2.002%	1.996%	1.955%	1.954%	**1.597%**
May	3.499%	2.309%	2.435%	**1.733%**	1.970%
Jun.	1.936%	2.075%	1.711%	1.728%	**1.315%**
Jul.	3.381%	1.927%	1.808%	1.892%	**1.348%**
Aug.	3.501%	2.563%	2.576%	2.559%	**1.900%**
Sep.	1.998%	2.003%	2.217%	2.347%	**1.967%**
Oct.	4.191%	**2.564%**	**2.494%**	3.410%	2.735%
Nov.	3.520%	2.685%	2.409%	2.771%	**1.899%**
Dec.	2.389%	2.112%	1.993%	2.105%	**1.654%**
Average	3.016%	2.257%	2.233%	2.355%	**1.935%**

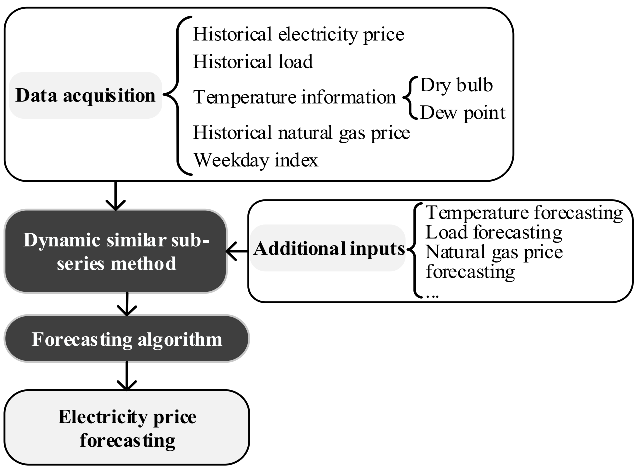

FIGURE 8. Electricity price forecasting model.

Future temperature, load and natural gas price can be regarded as the additional inputs.

The fuzzy similarity matrix R formed by each sub-series is shown as follows:

$$\mathbf{R} = \begin{pmatrix} 1 & 0.576 & 0.633 & 0.032 & 0.060 \\ 0.576 & 1 & 0.029 & 0.195 & 0.076 \\ 0.633 & 0.029 & 1 & 0.042 & 0.030 \\ 0.032 & 0.195 & 0.042 & 1 & 0.913 \\ 0.060 & 0.076 & 0.030 & 0.913 & 1 \end{pmatrix} \tag{22}$$

The result for each of the weights calculated by the fuzzy clustering method is shown in Table 6.

The MAPE obtained for every month in 2008 is presented in Table 7. Although the ARIMA and the BPTT perform better than the proposed method in February 2008, and also the LM-NN, the BPNN and the BPTT have better forecasts in April 2008, the proposed method obtains better forecasts in most of the months. In addition, the proposed method is in a position to reduce the average MAPE to 7.278%.

The MAPE obtained for some specific days in 2008 is shown in Table 8. The proposed method outperforms both of the aforementioned methods in forecasting day-ahead electricity price.

TABLE 6. Weight for each parameters (electricity price).

β_0	β_1	β_2	β_3	β_4
0.5613	0.1942	0.215	0.0108	0.0202

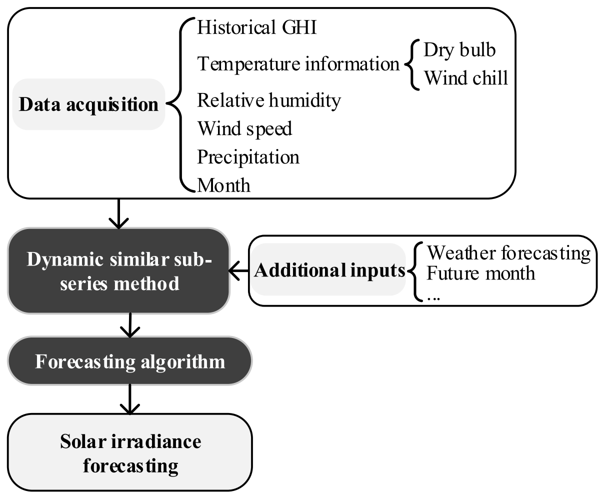

FIGURE 9. GHI forecasting model.

D. SOLAR IRRADIANCE FORECASTING

In radiometry, solar irradiance is the radiant power received by a surface per unit area. The GHI at 12 o'clock is one of the most important indicators for forecasting solar irradiance. In this case, day-ahead 12 o'clock GHI forecasting is performed. The structure of the GHI forecasting model is shown in Fig. 9.

In data acquisition, historical GHI, historical temperature (dry bulb and wind chill), relative humidity, wind speed, precipitation and month are comprised. Future temperature, relative humidity, wind speed, precipitation and month can be regarded as the additional inputs.

TABLE 7. Monthly MAPE in 2008 (electricity price).

Month	ARIMA	LM-NN	BPNN	BPTT	Dynamic similar sub-series method
Jan.	13.277%	13.776%	12.501%	10.782%	**10.565%**
Feb.	**9.534%**	10.501%	10.587%	**8.607%**	10.271%
Mar.	8.595%	8.435%	7.466%	8.512%	**4.291%**
Apr.	8.180%	**6.660%**	**7.120%**	**6.554%**	7.310%
May	7.809%	8.435%	6.883%	6.079%	**5.882%**
Jun.	6.662%	7.968%	7.822%	7.158%	**5.493%**
Jul.	10.692%	8.552%	8.411%	10.694%	**4.948%**
Aug.	14.524%	12.576%	12.009%	13.601%	**10.192%**
Sep.	8.913%	8.236%	7.794%	9.350%	**7.202%**
Oct.	9.289%	7.248%	8.578%	7.806%	**5.991%**
Nov.	17.816%	9.906%	8.801%	7.952%	**5.188%**
Dec.	13.077%	12.591%	13.077%	11.287%	**10.007%**
Average	10.697%	9.574%	9.254%	9.032%	**7.278%**

TABLE 8. MAPE for some days in 2008 (electricity price).

Day	ARIMA	LM-NN	BPNN	BPTT	Dynamic similar sub-series method
15th Feb.	11.077%	11.208%	12.083%	11.735%	**10.964%**
9th Jun.	5.819%	7.746%	8.552%	7.319%	**4.971%**
20th Aug.	15.298%	12.376%	11.997%	12.103%	**9.183%**
3rd Nov.	14.226%	8.519%	8.414%	7.931%	**6.194%**
Average	11.605%	9.962%	10.262%	9.772%	**7.828%**

TABLE 9. Weight for each parameters (GHI).

Parameter	Weight	Parameter	Weight
β_0	0.4952	β_4	0.0456
β_1	0.1176	β_5	0.0272
β_2	0.1174	β_6	0.0361
β_3	0.1609		

The fuzzy similarity matrix **R** formed by each sub-series is shown in (23) at the bottom of this page. The result for each of the weights calculated by the fuzzy clustering method is shown in Table 9.

The MAPE obtained for every month in 2014 is presented in Table 10 and Fig. 10. It can be observed that the proposed method has the best performance in eight months (out of twelve months). In addition, compared with the second-best-performing BPTT, the proposed method has a considerable improvement of approximately 2% in the average MAPE. Therefore, remarkable enhancements can be observed from the proposed method in forecasting day-ahead GHI at 12 o'clock.

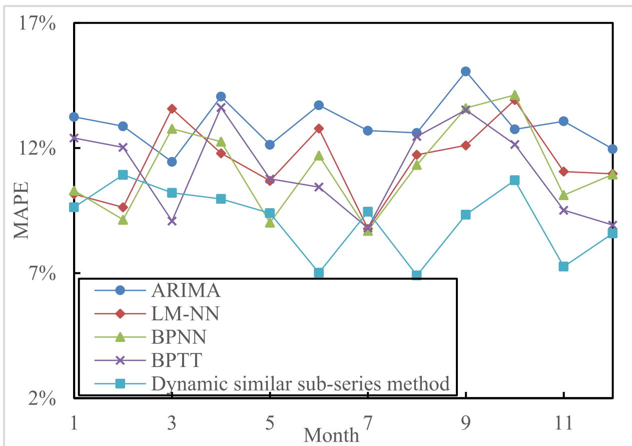

FIGURE 10. Monthly MAPE in 2014 (GHI).

Based on the cases above, the dynamic similar sub-series method can efficiently and accurately select the similar sub-series of the forecasting sub-series, thus can significantly improve the forecasting accuracy.

$$\mathbf{R} = \begin{pmatrix} 1 & 0.636 & 0.636 & -0.665 & 0.184 & -0.110 & -0.146 \\ 0.636 & 1 & 0.999 & -0.529 & 0.125 & -0.036 & 0.160 \\ 0.636 & 0.999 & 1 & -0.530 & 0.110 & -0.036 & 0.159 \\ -0.665 & -0.529 & -0.530 & 1 & -0.094 & 0.180 & 0.080 \\ 0.184 & 0.125 & 0.110 & -0.094 & 1 & -0.006 & -0.085 \\ -0.110 & -0.036 & -0.036 & 0.180 & -0.006 & 1 & 0.017 \\ -0.146 & 0.160 & 0.159 & 0.080 & -0.085 & 0.017 & 1 \end{pmatrix} \tag{23}$$

TABLE 10. Monthly MAPE in 2014 (GHI).

Month	ARIMA	LM-NN	BPNN	BPTT	Dynamic similar sub-series method
Jan.	13.242%	10.155%	10.296%	12.397%	**9.632%**
Feb.	12.869%	**9.630%**	**9.132%**	12.027%	10.928%
Mar.	11.446%	13.569%	12.767%	**9.083%**	10.209%
Apr.	14.054%	11.788%	12.254%	13.620%	**9.965%**
May	12.130%	10.688%	**9.015%**	10.765%	9.394%
Jun.	13.711%	12.778%	11.701%	10.439%	**7.011%**
Jul.	12.694%	**8.773%**	**8.691%**	**8.802%**	9.451%
Aug.	12.605%	11.729%	11.325%	12.461%	**6.905%**
Sep.	15.061%	12.104%	13.598%	13.525%	**9.335%**
Oct.	12.745%	13.920%	14.118%	12.142%	**10.710%**
Nov.	13.070%	11.059%	10.116%	9.512%	**7.257%**
Dec.	11.958%	10.969%	10.942%	8.917%	**8.586%**
Average	12.965%	11.430%	11.163%	11.141%	**9.115%**

V. CONCLUSION

The cumulative effect affects the accuracy of time series forecasting. In this paper, the dynamic similar sub-series method is proposed to select similar sub-series in order to address the cumulative effect. In the proposed method, the variation of target parameter sub-series and the variation of each influencing factor sub-series are innovatively integrated into the selection rules for the dynamic similar sub-series. The forecasting model proposed in this paper is applicable to the prediction of time series which are affected by the cumulative effect. Verification in different scenarios demonstrates that the forecasting accuracy is generally higher than the machine prediction level and almost approach the expert artificial prediction level. In addition, the forecasting method can not only be separately implemented for forecasting time series, but also can be used as a basis for the selection of similar time series and thus can be combined with other forecasting algorithms.

REFERENCES

[1] S. Fan and L. Chen, "Short-term load forecasting based on an adaptive hybrid method," *IEEE Trans. Power Syst.*, vol. 21, no. 1, pp. 392–401, Feb. 2006.

[2] T. V. Gestel *et al.*, "Financial time series prediction using least squares support vector machines within the evidence framework," *IEEE Trans. Neural Netw.*, vol. 12, no. 4, pp. 809–821, Jul. 2001.

[3] F. Martínez-Álvarez, A. Troncoso, G. Asencio-Cortés, and J. C. Riquelme, "A survey on data mining techniques applied to electricity-related time series forecasting," *Energies*, vol. 8, no. 11, pp. 13162–13193, 2015.

[4] L. Huang, Y. Yang, H. Zhao, X. Wang, and H. Zheng, "Time series modeling and filtering method of electric power load stochastic noise," *Protection Control Mod. Power Syst.*, vol. 2, no. 1, p. 25, 2017.

[5] E. Kayacan, B. Ulutas, and O. Kaynak, "Grey system theory-based models in time series prediction," *Expert Syst. Appl.*, vol. 37, no. 2, pp. 1784–1789, 2010.

[6] B. Li, J. Zhang, Y. He, and Y. Wang, "Short-term load-forecasting method based on wavelet decomposition with second-order gray neural network model combined with ADF test," *IEEE Access*, vol. 5, pp. 16324–16331, 2017.

[7] Y. Chen *et al.*, "Short-term load forecasting: Similar day-based wavelet neural networks," *IEEE Trans. Power Syst.*, vol. 25, no. 1, pp. 322–330, Feb. 2010.

[8] E. Paparoditis and T. Sapatinas, "Short-term load forecasting: The similar shape functional time-series predictor," *IEEE Trans. Power Syst.*, vol. 28, no. 4, pp. 3818–3825, Nov. 2013.

[9] P. Chen, T. Pedersen, B. Bak-Jensen, and Z. Chen, "ARIMA-based time series model of stochastic wind power generation," *IEEE Trans. Power Syst.*, vol. 25, no. 2, pp. 667–676, May 2010.

[10] K. Y. Chan, T. S. Dillon, and E. Chang, "An intelligent particle swarm optimization for short-term traffic flow forecasting using on-road sensor systems," *IEEE Trans. Ind. Electron.*, vol. 60, no. 10, pp. 4714–4725, Oct. 2013.

[11] Y. Liu, Y. Sun, D. Infield, Y. Zhao, S. Han, and J. Yan, "A hybrid forecasting method for wind power ramp based on orthogonal test and support vector machine (OT-SVM)," *IEEE Trans. Sustain. Energy*, vol. 8, no. 2, pp. 451–457, Apr. 2017.

[12] J. P. S. Catalão, S. J. P. S. Mariano, V. M. F. Mendes, and L. A. F. M. Ferreira, "Short-term electricity prices forecasting in a competitive market: A neural network approach," *Electr. Power Syst. Res.*, vol. 77, no. 10, pp. 1297–1304, 2007.

[13] O. Castillo and P. Melin, "Hybrid intelligent systems for time series prediction using neural networks, fuzzy logic, and fractal theory," *IEEE Trans. Neural Netw.*, vol. 13, no. 6, pp. 1395–1408, Nov. 2002.

[14] A. Bello, D. W. Bunn, J. Reneses, and A. Muñoz, "Medium-term probabilistic forecasting of electricity prices: A hybrid approach," *IEEE Trans. Power Syst.*, vol. 32, no. 1, pp. 334–343, Jan. 2017.

[15] H.-T. Yang, C.-M. Huang, Y.-C. Huang, and Y.-S. Pai, "A weather-based hybrid method for 1-day ahead hourly forecasting of PV power output," *IEEE Trans. Sustain. Energy*, vol. 5, no. 3, pp. 917–926, Jul. 2014.

[16] J. P. S. Catalao, H. M. I. Pousinho, and V. M. F. Mendes, "Hybrid wavelet-PSO-ANFIS approach for short-term electricity prices forecasting," *IEEE Trans. Power Syst.*, vol. 26, no. 1, pp. 137–144, Feb. 2011.

[17] J. Shi, J. Guo, and S. Zheng, "Evaluation of hybrid forecasting approaches for wind speed and power generation time series," *Renew. Sustain. Energy Rev.*, vol. 16, no. 5, pp. 3471–3480, 2012.

[18] M. Zhou and M. Jin, "Holographic ensemble forecasting method for short-term power load," *IEEE Trans. Smart Grid*, to be published. [Online]. Available: https://ieeexplore.ieee.org/document/8014465/

[19] N. Amjady and A. Daraeepour, "Midterm demand prediction of electrical power systems using a new hybrid forecast technique," *IEEE Trans. Power Syst.*, vol. 26, no. 2, pp. 755–765, May 2011.

[20] H. Quan, D. Srinivasan, and A. Khosravi, "Short-term load and wind power forecasting using neural network-based prediction intervals," *IEEE Trans. Neural Netw. Learn. Syst.*, vol. 25, no. 2, pp. 303–315, Feb. 2014.

[21] C. Wan, Z. Xu, Y. Wang, Z. Y. Dong, and K. P. Wong, "A hybrid approach for probabilistic forecasting of electricity price," *IEEE Trans. Smart Grid*, vol. 5, no. 1, pp. 463–470, Jan. 2014.

[22] Y.-Y. Hong and C.-P. Wu, "Day-ahead electricity price forecasting using a hybrid principal component analysis network," *Energies*, vol. 5, no. 11, pp. 4711–4725, 2012.

[23] Z. Tan, J. Zhang, J. Wang, and J. Xu, "Day-ahead electricity price forecasting using wavelet transform combined with ARIMA and GARCH models," *Appl. Energy*, vol. 87, no. 11, pp. 3606–3610, 2010.

[24] A. Kusiak, H. Zheng, and Z. Song, "Short-term prediction of wind farm power: A data mining approach," *IEEE Trans. Energy Convers.*, vol. 24, no. 1, pp. 125–136, Mar. 2009.

[25] N. Amjady, F. Keynia, and H. Zareipour, "Wind power prediction by a new forecast engine composed of modified hybrid neural network and enhanced particle swarm optimization," *IEEE Trans. Sustain. Energy*, vol. 2, no. 3, pp. 265–276, Jul. 2011.
[26] L. Yang, M. He, J. Zhang, and V. Vittal, "Support-vector-machine-enhanced Markov model for short-term wind power forecast," *IEEE Trans. Sustain. Energy*, vol. 6, no. 3, pp. 791–799, Jul. 2015.
[27] F. M. Alvarez, A. Troncoso, J. C. Riquelme, and J. S. A. Ruiz, "Energy time series forecasting based on pattern sequence similarity," *IEEE Trans. Knowl. Data Eng.*, vol. 23, no. 8, pp. 1230–1243, Aug. 2011.
[28] C. Li, P. Yang, W. Liu, D. Li, and Y. Wang, "An analysis of accumulative effect of temperature in short-term load forecasting," *Automat. Elect. Power Syst.*, vol. 33, no. 9, pp. 96–99, 2009.
[29] C. Li *et al.*, "Interaction between urban microclimate and electric air-conditioning energy consumption during high temperature season," *Appl. Energy*, vol. 117, no. 3, pp. 149–156, 2014.
[30] V. Martinez, G. I. Simari, A. Sliva, and V. S. Subrahmanian, "CONVEX: Similarity-based algorithms for forecasting group behavior," *IEEE Intell. Syst.*, vol. 23, no. 4, pp. 51–57, Jul. 2008.
[31] N. R. Pal and J. C. Bezdek, "On cluster validity for the fuzzy c-means model," *IEEE Trans. Fuzzy Syst.*, vol. 3, no. 3, pp. 370–379, Aug. 1995.
[32] J.-P. Mei, Y. Wang, L. Chen, and C. Miao, "Large scale document categorization with fuzzy clustering," *IEEE Trans. Fuzzy Syst.*, vol. 25, no. 5, pp. 1239–1251, Oct. 2017.
[33] G. Sidorov, A. Gelbukh, H. Gómez-Adorno, and D. Pinto, "Soft similarity and soft cosine measure: Similarity of features in vector space model," *Comput. Sistemas*, vol. 18, no. 3, pp. 491–504, 2014.
[34] A. J. Conejo, M. A. Plazas, R. Espinola, and A. B. Molina, "Day-ahead electricity price forecasting using the wavelet transform and ARIMA models," *IEEE Trans. Power Syst.*, vol. 20, no. 2, pp. 1035–1042, May 2005.
[35] Z. Ming-Guang and L. Lin-Rong, "Short-term load combined forecasting method based on BPNN and LS-SVM," in *Proc. IEEE Power Eng. Automat. Conf.*, Sep. 2011, pp. 319–322.
[36] P. J. Werbos, "Backpropagation through time: What it does and how to do it," *Proc. IEEE*, vol. 78, no. 10, pp. 1550–1560, Oct. 1990.
[37] ISO New England Inc. Accessed: Jun. 9, 2018. [Online]. Available: http://www.iso-ne.com
[38] *Nevada Power: Clark Station*. Accessed: Jun. 9, 2018. [Online]. Available: http://dx.doi.org/10.5439/1052547

PEIQIANG LI received the B.S. degree from Changsha Electric Power University, Changsha, China, in 1997, and the M.S. and Ph.D. degrees from Hunan University in 2004 and 2009, respectively, all in electrical engineering. He is currently an Associate Professor with Hunan University. His research interests include smart grid, load modeling, and electric power automation.

JIANG ZHANG was born in Tongling, Anhui, China, in 1993. He received the B.E. degree in electrical engineering from Hunan University, Changsha, China, in 2015, where he is currently pursuing the M.S. degree with the College of Electrical and Information Engineering. His major research interests include power grid planning and load forecasting.

CANBING LI (M'06–SM'13) was born in Yiyang, Hunan, China, in 1979. He received the B.S. and Ph.D. degrees in electrical engineering from Tsinghua University, Beijing, China, in 2001 and 2006, respectively. He is currently a Professor with the College of Electrical and Information Engineering, Hunan University, Changsha, China. His research interests include smart grid, energy efficiency, and energy policy.

BIN ZHOU (S'11–M'13–SM'17) was born in Hengyang, Hunan, China, in 1984. He received the B.S. degree in electrical engineering from Zhengzhou University, Zhengzhou, China, in 2006, the M.S. degree in electrical engineering from the South China University of Technology, Guangzhou, China, in 2009, and the Ph.D. degree from The Hong Kong Polytechnic University, Hong Kong, in 2013. He was a Research Associate and subsequently a Post-Doctoral Fellow with the Department of Electrical Engineering, The Hong Kong Polytechnic University. He is currently an Associate Professor with the College of Electrical and Information Engineering, Hunan University, Changsha, China. His main fields of research include smart grid operation and planning, renewable energy generation, and energy efficiency.

YONGJUN ZHANG received the B.E. and Ph.D. degrees in electrical engineering from the South China University of Technology, Guangzhou, China, in 1995 and 2004, respectively. From 1995 to 2005, he was a Research Assistant with the School of Electric Power, South China University of Technology, Guangzhou, an Assistant Professor from 2006 to 2013, and has been a Professor since 2013. He has authored three books and over 100 articles. His research interests include power system reactive power optimization, distributed generation control and optimization, voltage control, energy saving, and high-voltage direct current transmission.

MANMAN ZHU was born in Shangqiu, Henan, China, in 1991. She received the B.S. degree in electrical engineering from Zhengzhou University, Zhengzhou, China, in 2016. She is currently pursuing the M.S. degree with the College of Electrical and Information Engineering, Hunan University, Changsha, China. Her major research interests include new energy and short circuit current.

NING LI was born in Hengyang, Hunan, China, in 1995. He received the B.S. degree in electrical engineering from Hunan University, Changsha, China, in 2017, where he is currently pursuing the M.S. degree with the College of Electrical and Information Engineering. His major research interests include power grid planning and demand response.